

Moments and power generated by the horse (*Equus caballus*) hind limb during jumping

Darren J. Dutto^{1,*}, Donald F. Hoyt², Hilary M. Clayton³, Edward A. Cogger⁴ and Steven J. Wickler⁴

¹Department of Kinesiology and Health Promotion, California State Polytechnic University, Pomona, CA 91768, USA, ²Department of Biological Sciences, California State Polytechnic University, Pomona, CA 91768, USA, ³College of Veterinary Medicine, Michigan State University, East Lansing, MI 48824, USA and ⁴Department of Animal and Veterinary Science, California State Polytechnic University, Pomona, CA 91768, USA

*Author for correspondence (e-mail: ddutto@csupomona.edu)

Accepted 17 November 2003

Summary

The ability to jump over an obstacle depends upon the generation of work across the joints of the propelling limb(s). The total work generated by one hind limb of a horse and the contribution to the total work by four joints of the hind limb were determined for a jump. It was hypothesized that the hip and ankle joints would have extensor moments performing positive work, while the knee would have a flexor moment and perform negative work during the jump. Ground reaction forces and sagittal plane kinematics were simultaneously recorded during each jumping trial. Joint moment, power and work were determined for the metatarsophalangeal (MP), tarsal (ankle), tibiofemoral (knee) and coxofemoral (hip) joints. The hip, knee and ankle all flexed and then extended and the MP extended and then flexed during ground contact. Consistent with our hypothesis, large extensor moments were observed at the hip and ankle joints and large flexor moments at the knee and MP joints throughout ground contact of the hind limb. Peak moments tended to occur earlier in stance in the proximal joints but peak power generation of the hind limb joints occurred at similar times except for the MP joint, with the hip and ankle

peaking first followed by the MP joint. During the first portion of ground contact ($\approx 40\%$), the net result of the joint powers was the absorption of power. During the remainder of the contact period, the hind limb generated power. This pattern of power absorption followed by power generation paralleled the power profiles of the hip, ankle and MP joints. The total work performed by one hind limb was 0.71 J kg^{-1} . Surprisingly, the knee produced 85% of the work (0.60 J kg^{-1}) done by the hind limb, and the positive work performed by the knee occurred during the first 40% of the take-off. There is little net work generated by the other three joints over the entire take-off. Velocity of the tuber coxae (a landmark on the pelvis of the animal) was negative (downward) during the first 40% of stance, which perhaps reflects the negative work performed to decrease the potential energy during the first 40% of contact. During the final 60% of contact, the hip, ankle and MP joints generate positive work, which is reflected in the increase of the animal's potential energy.

Key words: horse, jumping, hind limb, knee joint, work, power, moment, ground reaction force, sagittal plane kinematics.

Introduction

The total work generated by a quadruped necessary to clear an obstacle during jumping would be generated by both the fore and hind limbs. For the horse, the forelimb has been found to create a greater ground impulse, but one of the primary determinants of success of a jump is the final push-off by the hind limbs (van den Bogert et al., 1994; Barrey and Galloux, 1997). The purpose of the present study was to determine the total work generated by the hind limb during the take-off of a jump. Further, it was our intention to determine the contribution of the hip, knee, ankle and MP (metatarsophalangeal) joints to the total work generated by the hind limb.

During a jump that requires both horizontal and vertical

displacement of the center of mass, it has been hypothesized that, for a quadruped, the resulting ground reaction force (GRF) generated by the hind limb would be anterior (or cranial) to the limb, implying that this force vector would be in front of the knee, which is the most anterior joint of the limb (van Ingen Schenau and Bobbert, 1993). A GRF vector cranial to the knee has been observed experimentally in a horse jumping over a 0.75 m barrier (Biewener et al., 1988). If the GRF vector is anterior to the knee, a net flexor moment is generated at the knee, while extensor moments would be observed at the hip and ankle (the hip, knee and ankle are joints with muscle able to produce significant work in the hind limb; Biewener, 1998).

It might be expected that the more proximal joints, with muscles able to generate work, would contribute the most to total work. This would certainly be true of the hip and ankle of the horse, since they should have net extensor muscle moments as hypothesized by van Ingen Schenau and Bobbert (1993) and as shown from the observed force vector by Biewener et al. (1988). In order to produce a GRF vector in front of the knee, a net flexor moment would be generated at the knee such that negative work would be done (due to knee extension during the take-off). The MP should contribute little to the total work as it is primarily controlled by small muscles and connective tissue (ligaments and long tendons). We test these ideas here by determining the work generated by the total hind limb in relation to the joint moments and powers produced at the hip, knee, ankle and MP joints for horses jumping over a barrier of moderate height (0.63 m).

Materials and methods

Animals and experimental protocol

Five horses (three Arabians and two Thoroughbreds; mean age, 8 ± 4 years) with a mean body mass of 491 ± 52 kg performed the experimental protocol, approved by the University's Animal Care and Use Committee. Each horse was exercised regularly and was free from injury that might affect jumping performance. Subject animals were trained to perform a jump for this study but were not bred specifically or conditioned for jumping over a long period of time. After a brief warm-up, each horse was prepared for data collection by placing retroreflective markers on appropriate hind limb landmarks using a cyanoacrylate adhesive. Markers were placed so that the hip, knee, ankle and metatarsophalangeal (MP) joints of the right hind limb could be identified (Fig. 1). Prior to the recording of any jumps, a video record was made of the horse in a 'standing square' position, defined when the metatarsal was in a perpendicular plane to the substrate and situated approximately in the middle of the force platform. Coordinate data developed from this control position were used to develop a segment model of the hind limb, which was important for determination of the location of the femorotibial and hip joints (see 'Determination of coordinates for the knee and hip joints' below).

A jumping barrier of modest height (0.63 m) was placed next to a force-measuring platform located in a runway. For each jumping trial, an animal trainer led the horse at a speed that produced a trot during the approach to the barrier. The animal trainer used a combination of a long tether and forward motion to allow the horse freedom of movement during and after the jump so as to not alter the horse's jumping behavior. Both force and video records were made of each jumping trial. Data for each trial were considered viable if only the right hind limb was on the force plate during the jump.

Determination of coordinates for the knee and hip joints

A significant amount of soft tissue is located over both the knee and hip joints of the hind limb and, while retroreflective

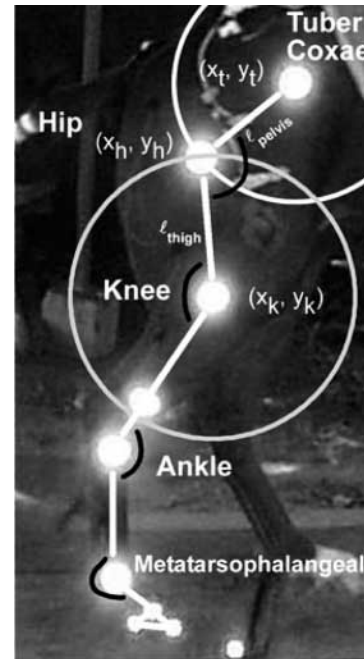


Fig. 1. The picture shows the reflective marker set-up with four joints of the hind limb. The locations of the knee and hip joints were mathematically determined using the geometrical relationships of the limb segments. Digitized coordinates were used to determine the knee, and the mathematically derived coordinates of the knee and the digitized coordinates of the tuber coxae were used to calculate the hip coordinate (see Materials and methods). The location of the hip (x_h, y_h) was determined using the coordinates of the knee (x_k, y_k) and tuber coxae (x_t, y_t), and the lengths of the pelvis (l_{pelvis}) and thigh (l_{thigh}) segments. If two circles are drawn with the tuber coxae and knee joint as origins and radius equivalent to the length of the appropriate segments, there will be two places where the circumferences of the circles overlap (or one if the segments are oriented in a straight line). The rearmost of these two intersections was taken as the location of the hip joint.

markers can be used to identify these joints, the soft tissue between the markers and the joint has been shown to impair the ability to determine joint location during movement (van Weeren et al., 1992; Back et al., 1995). In an attempt to reduce the error in determination of joint center location, the positions of these two joints were mathematically derived using additional markers placed over relatively stable anatomical locations (stable locations are defined as points where there is little intervening soft tissue between the skin surface and underlying bony structure).

The assumption was made that the segments that articulate in these joints maintain a constant length during the jump. The Cartesian coordinates for the knee joint were determined by using the geometric relationship between the shaft of the tibia, ankle joint and knee joint. Markers along the shaft of the tibia (ankle joint and tibial midshaft) formed a straight line representing the tibia. A polar coordinate relationship was determined (angle and radius) relative to the tibial markers using the ankle joint as the vertex of the angle representing the

tibia and an imaginary line from the ankle joint to the knee joint. Knowing the distance and angle of the knee point relative to the tibial markers allowed for the calculation of the Cartesian coordinates of a corrected knee joint location, regardless of the orientation of the tibia.

The hip joint was located by using the calculated Cartesian coordinates for the knee joint, the Cartesian coordinates for the pelvic marker and the lengths of the thigh and pelvic segments determined from the standing-square recordings. It was assumed that the length of each segment described a radius of a circle centered upon the segment end farthest from the hip joint (the knee and the tuber coxae; Fig. 1). The circumferences of the two circles intersect at two places, the rearmost of which was the location of the hip joint center. The Cartesian coordinates for the position where the two circles intersect were then calculated using the equations that described the two circles.

Experimental apparatus

A 0.6 m×0.9 m force plate (model 9287BA; Kistler Instruments, Winterthur, Switzerland) was used for all data collection. The force plate was situated lengthwise in the middle of a runway. The runway consisted of a cement base covered with a 10 mm-thick, high-density, black rubberized mat. The rubberized mat was also placed on the surface of the force plate. Covering the surface of the force plate with the rubberized mat created a continuous visual field for the horse, avoiding any reluctance on the part of the animal to approach and perform the jump. Force data were sampled at a rate of 1000 Hz for all tests. Force data were synchronized with high-speed video recording using LabView® (v5.1, National Instruments Inc., Austin, TX, USA), which generated a pulse to initiate simultaneous recording of both the force and video data. Center of pressure was calculated from the force data with a correction for the addition of the rubber matting to the surface of the force plate. To ensure the validity of calculated center of pressure coordinates, manual tests were performed by applying point loads to the surface of the force plate at a variety of angles and positions. Center of pressure was determined within 0.5 cm regardless of the direction that the load was applied to the surface of the force plate.

Video records of all jumping trials were obtained using a high-speed (250 Hz) digital camera (PCI 250; Redlake Imaging Corp., San Diego, CA, USA). The camera was situated orthogonal to the plane of movement, at a distance of 8 m, so that approximately 3.5 m of the runway were recorded, including the force platform and the jump barrier. Prior to experimental testing, a 48-point, two-dimensional calibration frame, located in the plane of movement over the force plate, was recorded. Video records of two-dimensional (sagittal plane) motion for kinematic analysis were recorded and stored directly to a computer. Limb segment

markers were digitized using the automatic point-tracking module of the Peak Motus® software (Peak Performance Technologies, Inc., Denver, CO, USA). Digitized coordinates were scaled to represent real-world Cartesian values using a two-dimensional Direct Linear Transformation constructed with the recorded calibration parameters. Kinematic coordinate data were smoothed with a dual pass fourth order Butterworth digital filter using a cut-off frequency of 20 Hz.

Data calculations

Angular positions for each joint were determined from the Cartesian coordinates of the hind limb joints. Linear position and velocity of the tuber coxae were determined from kinematic data. Moments and powers for each joint were determined using inverse dynamic analysis (Winter, 1990). Inertial properties of the hind limb segments were estimated using published equations (Buchner et al., 1997). The equations presented by Buchner et al. represent data for Dutch Warmblood horses. Using these equations, the assumption is made that the proportional relationship between the mass of the animal and the mass of the segments is similar between the Dutch Warmblood horses and the horses used in this study. While this relationship may not necessarily hold true, the effect of inertial properties of the limb segments relative to ground contact forces are relatively small; thus, discrepancies due to breed of horse on inertial properties of the hind limb segments should have a negligible influence on measured results during the stance phase of the jump. Fig. 2 displays both the total joint moment and the inertial moment due to the mass and moment of inertia of each segment for one jumping trial (which is representative of all trials). It is readily apparent that the contribution of the inertial properties to the total joint moment is rather small; thus, errors due to the estimation of these properties will not greatly influence the results of this study.

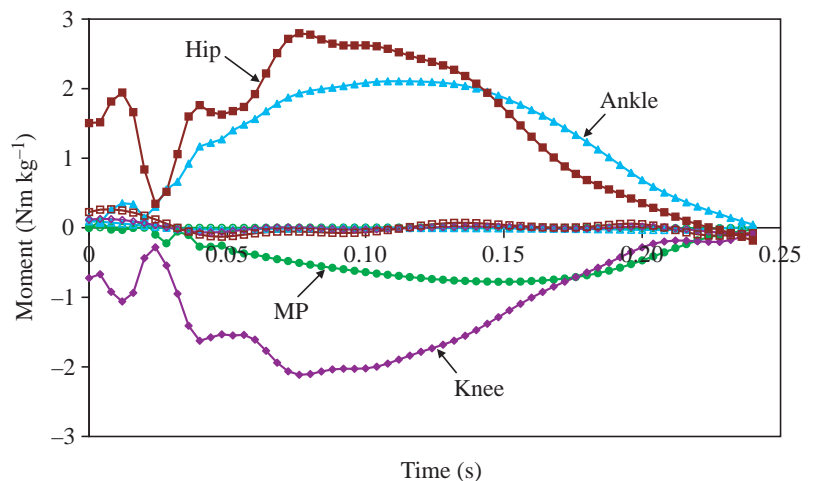


Fig. 2. Representation of the inertial moment relative to the joint moments for one jumping trial. The solid symbols are the total joint moment for each identified joint. The open symbols represent the inertial moments. Notice that the inertial moments are clustered near zero throughout the trial. MP, metatarsophalangeal joint.

Total power generated by the hind limb was determined by summing the power of the four joints at each relative time point. Finally, work performed by the joint was determined by integrating the power curves.

Collected data are descriptive; therefore, results are presented as means \pm S.D. Moment and power values are presented relative to body mass. Ensemble averaging was used to combine trial results across the five test animals for the purposes of presenting results (the number of jumps used in this analysis ranged from five to eight jumps per horse, all for the same barrier height, for a total of 29 jumping trials). Reported peak values represent an average of the peak

values taken from each individual trial for the particular parameter.

Results

Calculated joint moment patterns for all five animals tended to follow similar patterns, as illustrated by the observed averaged moments at the hip for each animal (Fig. 3A). Because the patterns were similar across animals, joint moments were averaged together and presented as means \pm S.D. (Fig. 3B). The GRF generated by the hind limb was in front of (anterior to) the limb for a majority of stance. The force would be generated by net extensor moments of the musculature of the hip and ankle joints and flexor moments by the musculature of the knee and MP joints. Peak extensor moments of the hip and ankle joints (2.6 Nm kg^{-1} and 2.2 Nm kg^{-1} , respectively) were generally larger than the peak flexor moments of the knee and MP joints (1.9 Nm kg^{-1} and 1.0 Nm kg^{-1} , respectively; Table 1). Peak moments tended to progress temporally over the time of contact in a proximal-to-distal fashion across the joints (hip – 36%, knee – 30%, ankle – 43%, MP – 57% of contact time).

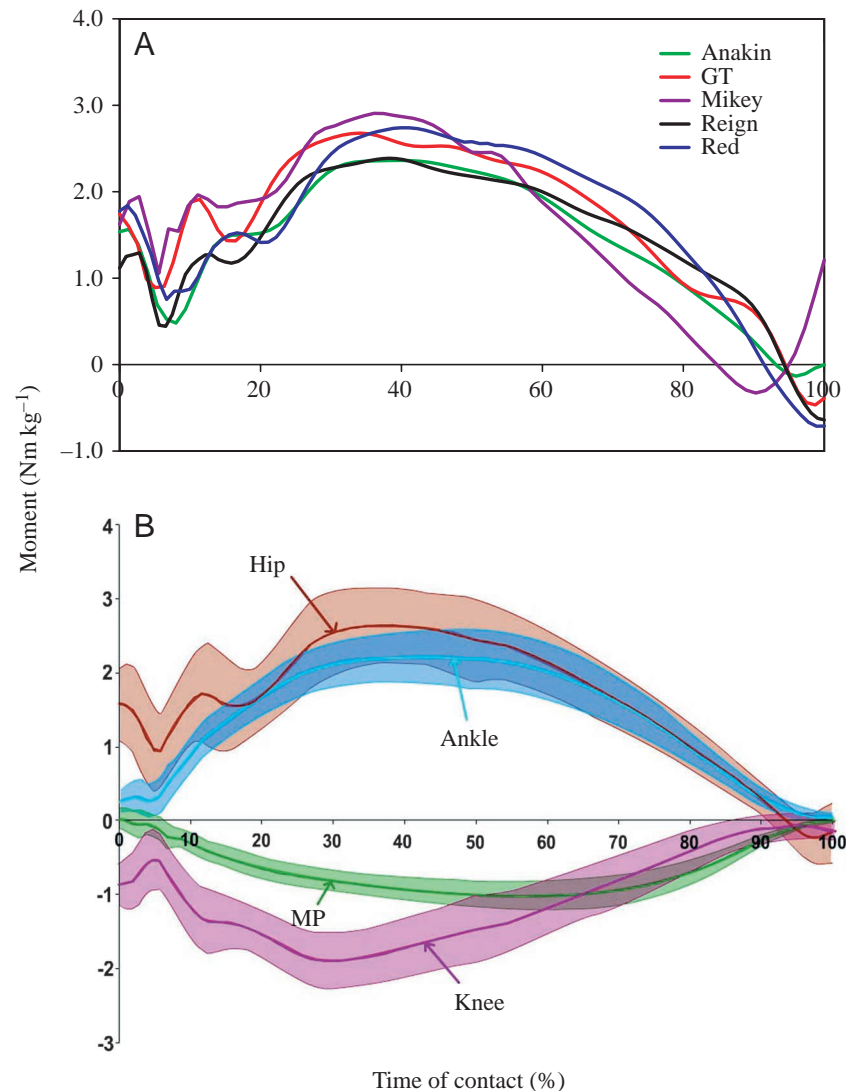


Fig. 3. Joint moments (relative to body mass) are presented. (A) Observed moments at the hip for each of the test animals. Each curve represents the mean of the trials for that animal, with the number of trials ranging between five and eight for the different animals. The five curves are very similar across animals. (B) Moments for the MP (metatarsophalangeal), ankle, knee and hip joints of the hind limb. Each curve represents the mean of 29 trials (solid line) \pm S.D. (shaded area) across all horses. For both plots, positive values represent extensor moments and negative values represent flexor moments for each joint.

All four joints had relatively large changes in angular position during ground contact (Fig. 4). The hip, knee and ankle joints all had a similar pattern of flexion followed by extension of the joint, whereas the MP joint behaved oppositely (hyperextension followed by flexion). For the MP joint, the effect of hyperextension during the early portion of stance is similar to the flexion that is occurring in the other joints, and this motion contributes to the overall shortening of the hind limb during this portion of stance. Subsequent flexion of the MP would then contribute to the lengthening of the limb during the latter part of stance. The average range of motion (ROM) was largest for the MP ($41.3 \pm 9.1^\circ$), followed by the knee ($33.8 \pm 11.9^\circ$), ankle ($29.4 \pm 7.2^\circ$) and hip ($24.9 \pm 6.3^\circ$). Maximal flexion was reached first in the hip and ankle joints, then by the MP joint (or maximum hyper-extension) and finally the knee joint (Table 1). These values appear consistent with kinematic results presented by van den Bogert et al. (1994).

The hip and ankle joints exhibited early power absorption followed by power generation (Fig. 5). Both of these joints became power generators for take-off, beginning around 45% of ground contact. For both the hip and ankle joints, average power absorption peaked at approximately 7 W kg^{-1} (Table 1), at 22% (ankle) and 28% (hip) of ground contact.

Table 1. Summary of joint kinematics and kinetics

Joint	ROM (deg.)	Relative time (%)	Peak moments (Nm kg ⁻¹)	Peak power (W kg ⁻¹)		Total work (J kg ⁻¹)	Work (%)	Work 40% (J kg ⁻¹)	Work 60% (J kg ⁻¹)
				Absorption	Generation				
MP	41.3±9.1	57±20	-1.02±0.19	-2.83±1.79	5.60±3.57	0.06±0.11	9	-0.13±0.13	0.20±0.11
Ankle	29.4±7.2	48±7	2.21±0.36	-6.80±2.53	7.44±4.28	0.03±0.36	5	-0.50±0.19	0.53±0.30
Knee	33.8±11.9	63±11	-1.90±0.38	-2.12±2.28	8.15±3.28	0.60±0.36	85	0.60±0.19	0.00±0.23
Hip	24.9±6.3	48±12	2.64±0.52	-7.23±4.13	5.72±3.20	0.01±0.35	2	-0.37±0.20	0.38±0.28
Sum						0.71±0.38	100	-0.40±0.15	1.11±0.38

The highest peak power generation was observed at the knee. The knee also did the most work on the center of mass over the entire ground contact, and all of that work was performed during the first 40% of ground contact. Additionally, range of motion (ROM) during ground contact in degrees and the time to the minimum (maximum for the ankle) as a percentage of ground contact are presented. Peak moments are presented for each joint, with the ankle and hip joints having predominantly extensor (positive value) moments and the MP (metatarsophalangeal) and knee joints having predominantly flexor (negative value) moments. All values are means ± s.d.

The MP joint also had slight power absorption for the initial 65% of ground contact and then became a power generator during the last 35% of ground contact. The amount of power absorption by the MP was relatively small compared with that of the ankle and hip joints. Mean peak power generation of 7.4 W kg⁻¹ and 5.7 W kg⁻¹ (Table 1) by the ankle and hip joints, respectively, occurred at 69% of ground contact for both joints. Peak power generation of 5.6 W kg⁻¹ (Table 1) by the MP joint occurred later (at 82% of ground contact) than that of the hip and ankle joints. The knee joint generated power during initial contact until 57% of ground contact and then absorbed energy. Power generation across the knee peaked at 8.2 W kg⁻¹ (Table 1) at 27% of ground contact time. During the latter portion of ground contact, the amount of power absorbed by the knee remained relatively small. During some trials, the knee joint behaved as a power generator during the latter portion of ground contact, as evidenced by the s.d. of the presented curve (Fig. 5).

On average, there was net negative power (or absorption of power) by the hind limb during the first 40% of ground contact, and net positive power (or power generation) for the remainder of ground contact (Fig. 6). Mean peak power generation of the hind limb was 13.2 W kg⁻¹ at 74% of ground contact. On average, one hind limb generated 0.71 J kg⁻¹ of work during ground contact. Over the entire ground contact, all four joints had a net contribution of positive work, with most of the work produced by the knee joint (0.60 W kg⁻¹). When averaged across all trials, the knee was responsible for 85% of the observed work of the hind limb, followed in order by the MP, ankle and the hip joints, with the hip joint producing an average of 2% of the work of the hind limb.

During the first 40% of ground contact, the horizontal velocity of the tuber coxae first decreased and then increased to a value ~0.15 m s⁻¹ faster than at contact, and the vertical velocity went from a negative (downward) velocity to zero (Fig. 7). During this portion of ground contact, the knee produced a mean of 0.60 J kg⁻¹ of positive work, while the other three joints all produced negative work, with the net result being negative work (Table 1). During the last 60% of contact, the vertical velocity increased dramatically, while the

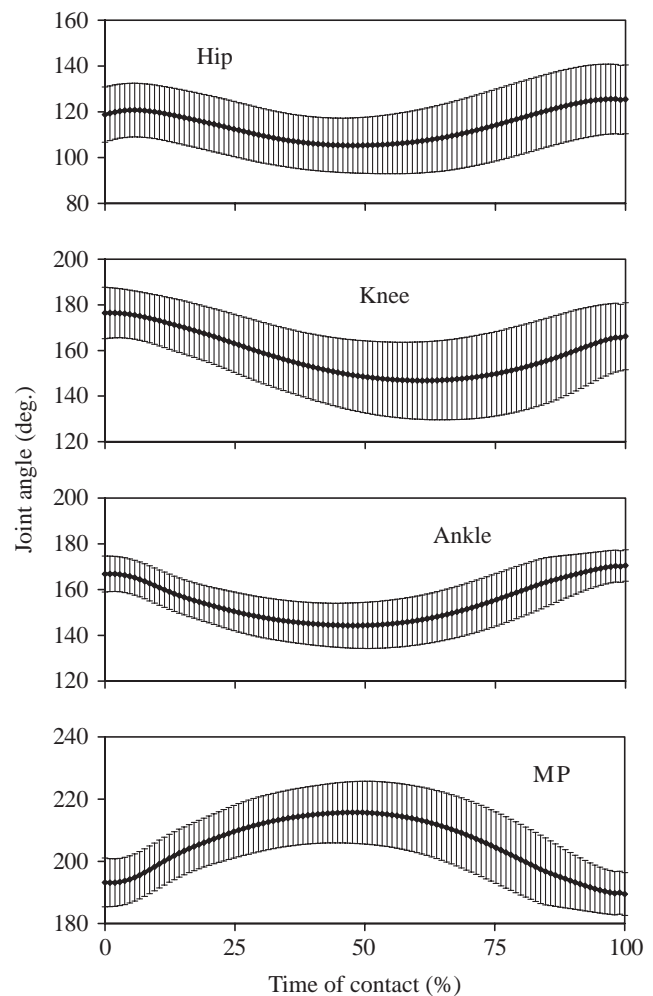


Fig. 4. Mean angular position data for all trials of the hind limb joints are presented (29 trials included in the mean). Each curve represents a mean (solid line) ± s.d. (crossbars) for the respective joint. Decreasing angles represent joint flexion and increasing angles represent joint extension. MP, metatarsophalangeal joint.

horizontal velocity increased slightly at the beginning and end of this time period. The knee produced essentially no work (on

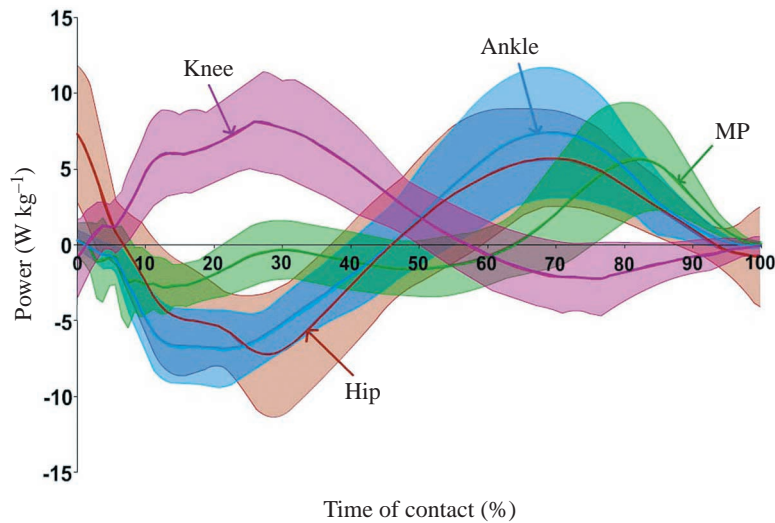


Fig. 5. Joint power (relative to body mass) for the MP (metatarsophalangeal), ankle, knee and hip joints of the hind limb during ground contact. Each curve is the mean of 29 trials (solid line) \pm s.d. (shaded area) of the power. Positive values represent power generation and negative values represent power absorption.

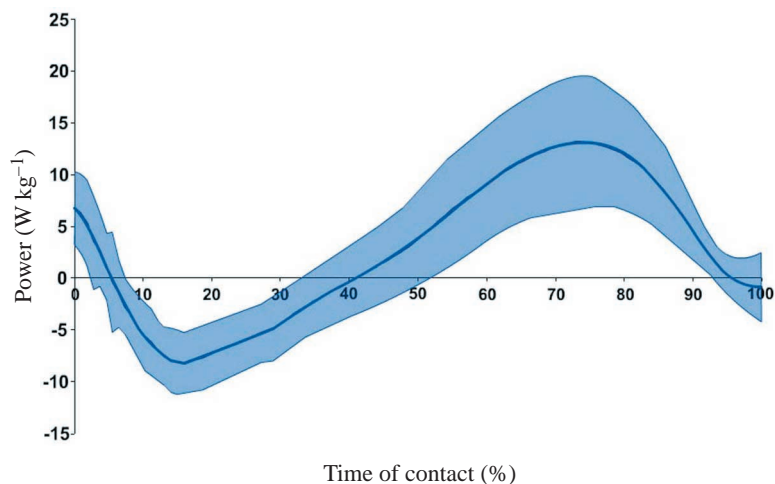


Fig. 6. Net power created by the hind limb during the jump. The curve represents the mean of 29 trials (solid line) \pm s.d. (shaded area) of the summed power from the four joints of the hind limb.

average) while the other three joints produced positive work during this time period.

Discussion

Our initial hypothesis of the direction of joint moments (hip and ankle – extensor moment; knee – flexor moment) based upon the work of van Ingen Schenau and Bobbert (1993) and the observations of Biewener et al. (1988) was confirmed. Furthermore, during ground contact of the hind limb for the take-off of a jump, the hip, knee and ankle joints underwent flexion followed by extension, while the MP extended and then flexed. Due to the moments generated at each joint and their

angular movement, work was performed primarily at the knee early in the ground contact and at the hip, ankle and MP joints during the latter part of contact. However, the knee produced a majority (85%) of the positive work, which was not necessarily expected from the hypothesis of van Ingen Schenau and Bobbert (1993).

For jumping horses in the present study, one hind limb generated an average of 0.71 J kg^{-1} of work (work was normalized to body mass). This is approximately 4.5 times the work of walking in horses (0.16 J kg^{-1} of work; Clayton et al., 2001). Peak extensor moments at the hip were five times higher during jumping (2.64 Nm kg^{-1}) than during walking (Clayton et al., 2001). Unexpectedly, positive work associated with the jump was done by the musculature of the knee rather than the hip or ankle joints. By contrast, during walking most of the work was performed by the hip (0.23 J kg^{-1}), which is greater than the total work done by the hind limb during walking, as the knee absorbs energy (produces negative work) during walking (Clayton et al., 2001).

The observed behavior of the knee joint was consistent with our hypothesis that the muscles acting at the knee would generate a flexor moment during jumping. This results in the GRF vector passing anterior to the knee during ground contact, similar to the observations of jumping horses made by Biewener et al. (1988). More interestingly, the knee generated positive work during the jump (rather than producing negative work, which we had hypothesized) and was the major (85%) contributor to the total work produced by the hind limb. Most of the power generation (positive work) at the knee occurred early (first 40%) in the contact period (Fig. 6), since this is when the knee was flexing and generating a flexor moment. How might the work generated by the knee contribute to the jump?

During the first 40% of stance, the knee musculature performed a majority of the positive work done during the entire contact period. Muscles of the other three joints were absorbing energy (performing negative work) during this same time period. From initial hoof contact to 40% of stance, the mean change in the resultant velocity of the tuber coxae was 0.04 m s^{-1} (Fig. 7), requiring 0.13 J kg^{-1} of work. During this time period, the work performed by the hind limb was -0.40 J kg^{-1} . The animals did increase the horizontal velocity of the tuber coxae by $\sim 0.15 \text{ m s}^{-1}$ over the first 40% of stance (Fig. 7) despite producing a braking force for the first 28% of stance (Fig. 8). The observed increase in horizontal velocity of the tuber coxae therefore is probably due to the positive work performed by the knee joint muscles during this time, because the muscles of the knee were the only muscles producing positive work. Furthermore, it is clear that during jumping a positive (propulsive) horizontal impulse is required, resulting

in half as much braking impulse as is generated during trotting [0.06 N s kg^{-1} (trotting) vs 0.03 N s kg^{-1} (jumping); Fig. 8]. As the braking period is very short during jumping, the force vector must be in front of the leg due to the joint moments generated during stance. The remaining joints were responsible for slowing the downward motion of the hips, resulting in the observed negative work performed by these joints. Without knowing the movement of the center of mass or the fore limbs, it is unclear exactly how the net negative work (-0.40 J kg^{-1}) performed by the hind limbs relates to the motion of the horse.

Another explanation for the relatively short braking period during the jump and the excess amount of work that appears at the knee during the first 40% of contact relates to the position of the torso of the horse (forelimbs off the ground) during the take-off. Since the tuber coxae is located on the pelvis, the horizontal velocity of this marker should provide a fairly good estimate of the horizontal velocity of the animal. There was a small discrepancy between the relationship of the early and large horizontal GRF and horizontal velocity. It is plausible that the extension moment of the hip acts primarily to provide propulsion for the jump and secondarily to assist in resisting the rotational inertia of the torso. During approximately 55–75% of contact, the hip was extending (Fig. 4) and the angular velocity was increasing, while the horizontal velocity of the tuber coxae was not increasing and there was a large, propulsive horizontal force. It appears that a small portion of the hip extension moment generated was required to resist the influence of gravity on the torso that would tend to flex the hip.

During the last 60% of contact, vertical velocity increased almost continually. The hip, ankle and MP joint all generated positive work during this time period that most likely acted to increase vertical velocity, while the knee musculature did not directly contribute to accelerating the animal. The positive work performed by the musculature of hip, ankle and MP joints was slightly greater than the amount of work absorbed during the initial portion of contact, an indication that the observed work was due to a combination of stored elastic energy recovery and active muscle contraction, as observed by Seyfarth et al. (2000) in human long jumping.

It seems possible that power produced by knee extensors was transferred to the hip and ankle by the action of the biarticular knee flexor muscles (e.g. hamstrings and gastrocnemius) that also act to extend the hip and ankle. Support for this idea is found in the similarity between the last 40% of the stance in equine jumping and part of the downstroke in human cycling, where, in both cases, a net flexor moment was generated at the knee while the hip, knee and ankle were all extending. When these conditions occur during human cycling there is co-activation of knee extensors and flexors and this has been interpreted as resulting in the transfer of work performed by the knee extensors to the hip and ankle (van Ingen Schenau, 1990; van Ingen Schenau et al., 1992, 1995). The fact that the knee

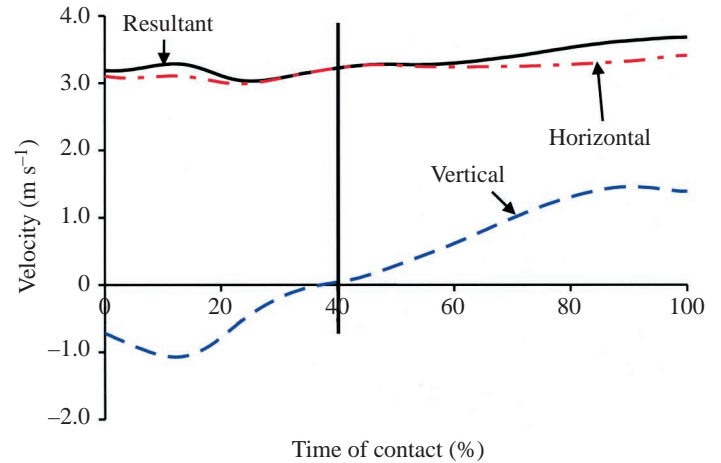


Fig. 7. During the first 40% of contact (when the total power is primarily negative), the mean horizontal velocity of the tuber coxae increased and the mean vertical velocity changed from negative to approximately 0. The resultant velocity remains essentially constant (the same value at the beginning and end of the time period) during the first 40% of contact. During the last 60% of contact, the horizontal velocity remains essentially constant until near the end, and the vertical velocity substantially increases; thus, the resultant velocity increases almost continuously over the final 60% of contact. 40% of contact is indicated by the vertical line. Velocity values represent the mean across all trials.

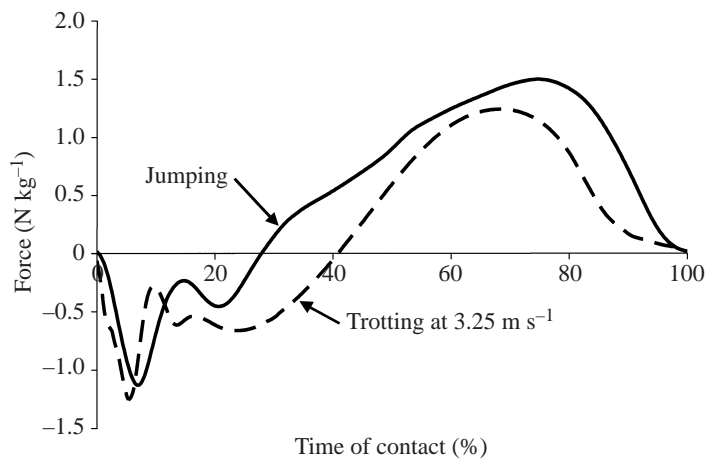


Fig. 8. The horizontal ground reaction force is only negative for the first 25% of ground contact, which means that the force vector stays anterior to the knee (the leg) throughout ground contact. Horizontal velocity decreases slightly during the first 25% of contact, which coincides with the negative (braking) horizontal force. For comparison, the mean horizontal force during trotting at 3.25 m s^{-1} (which is a speed very similar to mean speed during the jump) is shown. The amount of braking that occurs during trotting is greater (larger area) than during jumping. The braking impulse during trotting is roughly twice that of jumping (0.06 N s kg^{-1} vs 0.03 N s kg^{-1}). The curve represents the mean horizontal force for all trials.

extended during the later part of jumping suggests that knee extensors were active, and the very low power output of the knee during this phase of the jump, with concomitant increased

power production at the hip and ankle (Fig. 5), is consistent with the idea that power produced by knee extensors is transported to the hip and ankle. However, further investigation of the activity of the knee musculature (biarticular knee flexors and monoarticular knee extensors) during the jump is required to test this idea.

Towards the end of the take-off, positive work by the hind limb was maintained due to an increase in power generated by the MP joint. Positive work was not performed until 65% of contact in the MP joint, which acted to maintain the total positive power created by the hind limb. The MP joint does not have a large muscle mass acting across it but is primarily controlled by tendons attached to highly pinnate muscles with short fibers and by ligaments in the limb, similar to that described for the forelimb metacarpal-phalangeal joint (McGuigan and Wilson, 2003). Perhaps it is the late release of stored elastic energy that is responsible for some of the work observed in the MP joint during the final third of the take-off.

Late release of the energy in the MP joint may also be part of the proximal-to-distal flow of energy during take-off. During maximal vertical jumps, the extensor muscles of the hind limb in cats were found to activate in a proximal-to-distal order, and the kinematics of the hind limb joints followed the same proximal-to-distal pattern (Zajac et al., 1981). Also, the peak moments about these joints occurred earliest in the proximal joints during the jump. A similar pattern was observed in the peak moments generated by the hind limb joints of the horse during the jump, particularly when observing the relationship of the hip, ankle and MP joints. Additionally, the power generated by these joints tended to follow a similar pattern, with the peak power generation of the MP joint occurring later in stance than the hip and ankle joints. This proximal-to-distal sequencing of peak power would be indicative of energy transfer between the proximal joints (relatively large muscle mass) and the more distal joints. The tendinous nature of the MP joint is ideally designed for a late release of energy. As the force upon the joint decreases, this could allow tendon recoil and recovery of stored elastic energy. This is apparent in the late positive power burst observed at the MP joint.

Because the work done by the hind limb produced a large propulsive force during take-off, it can be argued that the hind limb performs a majority of the work required for the jump. The total proportion of work performed by the hind limb will not be known until the work performed by the forelimb and movement of the center of mass are determined. Most of the work was performed early during the stance phase by the musculature of the knee, as determined through inverse dynamic analysis. The hip, ankle and MP joint did a large amount of positive work later in stance but this was balanced

by negative work early in stance. Further investigation is required to determine how the positive work of the knee musculature contributes to the overall movement of the jumping animal and the proportion of the work produced by the hind limb relative to the total work required.

This study was funded by NIH grant # S06 GM53933 to D.F.H. and S.J.W. Horses were trained by Deborah Mead with the help of Shannon Garcia. We would also like to acknowledge Holly M. Greene, MS, Equine Research Technician, for providing technical support. We are grateful to an anonymous reviewer for suggestions that significantly strengthened this analysis.

References

- Back, W., Schamhardt, H. C., Savelberg, H. H. C. M., van den Bogert, A. J., Bruin, G., Hartman, W. and Barneveld, A. (1995). How the horse moves: 2. Significance of graphical representations of equine hind limb kinematics. *Equine Vet. J.* **27**, 39-45.
- Barrey, E. and Galloux, P. (1997). Analysis of the equine jumping technique by accelerometry. *Equine Vet. J. Suppl.* **23**, 45-49.
- Biewener, A. A., Thomason, J. J. and Lanyon, L. E. (1988). Mechanics of locomotion and jumping in the horse (*Equus*): *in vivo* stress in the tibia and metatarsus. *J. Zool. Lond.* **214**, 547-565.
- Biewener, A. A. (1998). Muscle function *in vivo*: a comparison of muscles used for elastic energy savings versus muscles used to generate mechanical power. *Am. Zool.* **38**, 703-717.
- Buchner, H. H. F., Savelberg, H. H. C. M., Schamhardt, H. C. and Barneveld, A. (1997). Inertial properties of Dutch Warmblood horses. *J. Biomech.* **30**, 653-658.
- Clayton, H. M., Hodson, E., Lanovaz, J. L. and Colborne, G. R. (2001). The hind limb in walking horses: 2. Net joint moments and joint powers. *Equine Vet. J.* **33**, 44-48.
- McGuigan, M. P. and Wilson, A. M. (2003). The effect of gait and digital muscle activation on limb compliance in the forelimb of the horse *Equus caballus*. *J. Exp. Biol.* **206**, 1325-1336.
- Seyfarth, A., Blickhan, R. and van Leeuwen, J. L. (2000). Optimum take-off techniques and muscle design for the long jump. *J. Exp. Biol.* **203**, 741-750.
- van den Bogert, A. J., Janssen, M. O. and Deuel, N. R. (1994). Kinematics of the hind limb push-off in elite show jumping horses. *Equine Vet. J. Suppl.* **17**, 80-86.
- van Ingen Schenau, G. J. (1990). On the action of biarticular muscles, a review. *Neth. J. Zool.* **40**, 521-540.
- van Ingen Schenau, G. J., Boots, P. J. M., Degroot, G., Snackers, R. J. and Vanwoensel, W. W. L. M. (1992). The constrained control of force and position in multijoint movements. *Neuroscience* **46**, 197-207.
- van Ingen Schenau, G. J. and Bobbert, M. F. (1993). The global design of the hind limb in quadrupeds. *Acta Anat.* **146**, 103-108.
- van Ingen Schenau, G. J., Dorssers, W. M. M., Welter, T. G., Beelen, A., Degroot, G. and Jacobs, R. (1995). The control of mono-articular muscles in multijoint leg extensions in man. *J. Physiol.* **484**, 247-254.
- van Weeren, P. R., van den Bogert, A. and Barneveld, A. (1992). Correction models for skin displacement in equine kinematic gait analysis. *J. Equine Vet. Sci.* **12**, 178-192.
- Winter, D. A. (1990). *Biomechanics and Motor Control of Human Movement*. 2nd edition. New York: John Wiley & Sons.
- Zajac, F. E., Zomlefer, M. R. and Levine, W. S. (1981). Hind limb muscular activity, kinetics, and kinematics of cats jumping to their maximum achievable heights. *J. Exp. Biol.* **91**, 73-86.